

# IMPLEMENTATION AND FLIGHT TESTING OF AN ENHANCED STABILITY SYSTEM FOR A VERY FLEXIBLE AIRCRAFT

Pedro J. González\*, Carlos E. S. Cesnik\*, Flávio J. Silvestre \*\*

\*University of Michigan, \*\*Instituto Tecnológico de Aeronáutica

**Keywords:** *Very Flexible Aircraft, Flight Test, Stability Augmentation System, Handling Qualities*

## Abstract

*A system to enhance stability based on proportional-integral controllers is investigated and demonstrated in flight for a very flexible aircraft. It was implemented on the X-HALE UAS testbed and flight tests were performed to quantify its performance and impact on the aircraft handling qualities. Based on pilot comments the handling qualities of the aircraft improved significantly compared to its original open-loop response.*

## 1 Introduction

Commercial and environmental requirements drive the development of more efficient aircraft. High-aspect-ratio wings designs are associated with reduced induced drag and, therefore, increased fuel efficiency. However, increase in structural weight must be mitigated for a net beneficial solution. This relation between high span wings and light structures leads to an increase in the structural flexibility [1]. One of the more significant characteristics of very flexible aircraft (VFA) is the low frequency of the structural modes and their coupling with the flight dynamics modes. The coupling of these frequencies can significantly impact the aircraft handling qualities, gust and maneuver load response, and flutter stability [1]. To understand the complex aeroelastic phenomenon on a VFA it is necessary to develop multi-disciplinary models that incorporate aerodynamics, inertial, and structural in-

teractions on a free flight condition. These formulations must be capable of capturing the various interactions exhibit by the system with different levels of flexibility and nonlinearities. However, before these new multi-disciplinary nonlinear formulations can be reliably used, their validation is required. While the various components of such formulation can be validated in isolation, the complex interactions of nonlinear aeroelasticity and flight mechanics can only be assessed in free flight. These make the validation process a complex task.

For the past 9 years, the Active Aeroelasticity and Structures Research Laboratory of the University of Michigan has been working on a testbed that can support code validation and development of control laws for VFA. The outcome of this effort is the experimental high-altitude long-endurance (X-HALE) radio-controlled testbed representative of a VFA [2]. It was conceived as an experiment to obtain fundamental nonlinear aeroelastic data to support validation of nonlinear aeroelastic-coupled-flight mechanics codes and serve also as a platform for control law studies. The data collected from this experiment will be used to support the validation of, among others, the University of Michigan's Nonlinear Aeroelastic Simulation Toolbox (UM/NAST) [3],[4]. While few requirements were imposed on its design, the resulting testbed should be able to capture unique coupled nonlinear aeroelasticity-flight dynamics interactions in very flexible aircraft not easily ob-

tained from wind tunnel tests. To that end, the X-HALE was designed to present an unstable Dutch-roll coupled with the first antisymmetric bending mode that is excited only under finite disturbances while undergoing large geometric wing deflections. That is, the vehicle is stable in calm air and under small disturbances but develops a coupled aeroelastic-flight dynamics instability in the presence of large disturbances. The X-HALE has undergone multiple phases of development for its airframe and instrumentation, all supported by ground and flight tests. This paper describes the implementation and evaluation of a linear (proportional-integral) controller to artificially enhance the stability of the aircraft, improving its handling qualities required for future flight tests with sensitive stereo-optical camera system.

## 2 The X-HALE Testbed

The remote-controlled X-HALE is a composite-built unmanned aircraft system (UAS) whose uniform EMX-07-airfoil wing is composed of six 1-m span panels with a 20-cm chord [2]. The X-HALE has five pods under the wing for the installation of the instrumentation and motors as shown in Fig. 1. It has also four horizontal elevons connected to the wing with booms, and spoilers in the external wing panels. The central tail is able to flip from vertical to horizontal position to vary yaw damping mechanically. The UAS is stable with this tail surface in the vertical orientation. During tests, the finite disturbance is induced by the step input in the spoilers, so to induce the unstable Dutch roll-antisymmetric bending mode. While the various elevons can be commanded independently, the current X-HALE configuration operates all of them together to control pitch; the spoilers differentially to control roll; the two outboard motors on each side linked together and operated in a differential way from each side of the vehicle are used to control yaw; and all motors together provide thrust.

As part of the X-HALE development and risk mitigation plan, two versions of UAS are carried out concomitantly: the Aeroelastic Test Vehicle

(ATV) and the Risk Reduction Vehicle (RRV). Both have the exact same inertia, elastic, and aerodynamic properties. The ATV is the fully instrumented version of the aircraft where the source data will be coming from. It contains a stereo-optical system to measure the deflection of the wing; inertial measurement units (IMU) in each external pod and an IMU/INS unit in the central pod; a pair of accelerometers at each wing tip; and three five-hole probes along the wing span. To process all this data, two computers are installed on board. The ATV also has communication to a ground station [5].

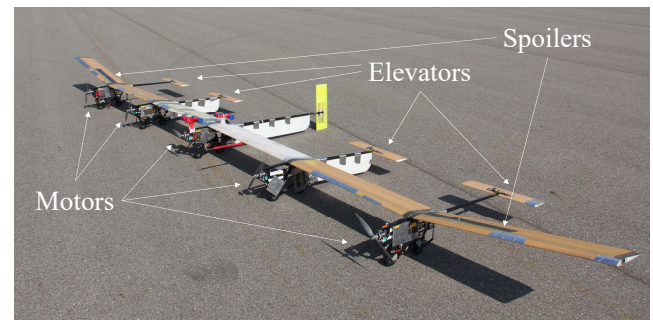


**Fig. 1** The X-HALE RRV on the ramp before flight.

To reduce development risk with this experimental platform, the RRV was conceived in parallel to the ATV. The RRV is as a lightly instrumented version of the ATV to be used to train pilots and ground station operators, as well as test new aircraft and control configurations before they are deployed to the ATV [6]. The RRV is instrumented with a PX4 PixHawk board in its central pod. PixHawk is an open source low-cost autopilot hardware. This computer board is integrated with a GPS/IMU and is capable of providing the rigid body motion of its location. The device also allows the connection of a pitot probe and is capable of connecting to a transmitter for live data monitoring in a ground station [7]. Figure 2 illustrates the hardware associated with the RRV for this study. The pilot is able to control the aircraft with an RC transmitter and with it, the pilot is capable of activating all the control effectors of the aircraft as well as insert doublets and frequency sweeps, with a code pre-programmed into the PixHawk. A ground station monitors the data

and adjust signals and gains through QGroundControl. QGroundControl is an open source code that allows operators to connect to any Mavlink enabled drone. The software has the capability to interact with PixHawk boards [8].

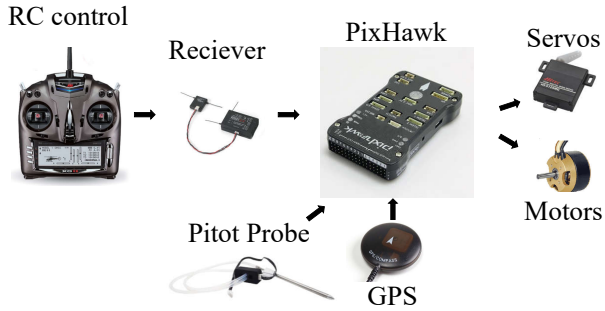


**Fig. 2** Simplified RRV autopilot and instrumentation used for the ESS flight tests.

As an instrument of risk mitigation, everything is tested on the RRV before it is installed on the ATV. The RRV is typically instrumented only on the central pod, and due to the lack of other electronics, ballast masses are added to the other pods to match the inertial and weight distribution of the ATV. The aircraft is able to display large wing tip displacements and poor handling qualities (HQ), as expected. Handling qualities are characteristics that govern the ease and precision with which a pilot is capable of performing a required task or mission depending on the aircraft [9]. A classical way to access the HQ of an aircraft is the Cooper-Harper rating scale. The application of this inquiry allows measuring the pilot's objective opinion and classify the performance of the aircraft. The pilot's evaluation of the baseline, open loop response of X-HALE is 9 (on a scale of 1 to 10) in the Cooper-Harper rating scale. This means that the aircraft is controllable, nevertheless, intense pilot compensation is required to retain control. This characteristic of the vehicle, although introduced intentionally in its design, makes the resulting aircraft very challenging to fly and land. However, due to the stereo-optical system fragility in operation and calibration, the ATV cannot afford be submitted to high landing loads that could misaligned the cameras and prevent an after-flight calibra-

tion verification, a procedure desirable to verify the quality of the deformation data measured during flight. Therefore, a temporary increase in stability is needed to safely position the testbed to collect data, at which point the artificial stability augmentation needs to be remove for the experiment to be conducted under the aircraft designed properties. The enhanced stability system (ESS) should then be re-engaged after the data collection is over and before bringing the airplane to land.

### 3 Description of the Enhanced Stability System

As expected, control laws for VFA based on only the rigid body approximation of the aircraft flight dynamics should not perform properly [10]. Nevertheless, Rona *et al* (2018) [11] and Pang (2018) [12] have numerically shown that it is possible to stabilize a VFA using only rigid body feedback when the overall dynamics of the aircraft is taken into account, at least for certain segments of the flight envelope. The X-HALE is operated by a (human) pilot and to achieve the experiment's main goal of acquiring the free flight dynamics coupled with the aeroelastic response, it is necessary to increase the controllability of the aircraft in order to reduce the pilot workload before taken data. The aircraft needs to take off and land with the ESS on to improve its HQ in the critical flight phases. This ESS also needs to be available after the experiments are conducted to return the aircraft to its trim condition. Finally, the ESS needs to be able to be deactivated during the signal injection to allow the open-loop response of the aircraft to develop. The pilot and/or the ground station can activate or deactivate the ESS. The ESS needs to be able to stabilize the aircraft only with rigid body states. This can be implemented in the PixHawk that is able to provide:

- Euler angles for pitch ( $\theta$ ), roll ( $\phi$ ) and yaw ( $\psi$ ) axes and their respective angular rates  $p$ ,  $q$  and  $r$ ;
- GPS position and velocity;

- Airspeed;
- Control surfaces commands.

Based on previous flights, Pang (2018) [12] was able to complete its open-loop system identification. Transfer functions (TF) that relate the actuators with the angular rates were developed from those tests. That effort also showed the ability of PI controllers as ESS on the three axes. The pitch controller, however, showed slow response and, therefore, degraded pitch axis performance [12].

Since previous flight campaigns demonstrated that the pilot had enough control authority on the pitch axis, the main problem was to stabilize the lateral-directional axes once the aircraft starts to develop an undamped Dutch roll with asymmetric wing bending coupling [6]. In this research, the ESS was focused on regulating the lateral-directional axes, while no regulation of the longitudinal axis was performed. The TF for the roll axis relates the deflection of the spoiler with the roll angular rate. The TF for the yaw axis relates the differential thrust with the yaw rate. To reduce the workload on the pilot, another loop was applied to the roll axis. The purpose of this loop is to track the roll angle and help the aircraft to return back to a leveled condition after disturbance. Due to the limited computational capabilities and sensors, a common SISO proportional-integral (PI) controller was used to stabilize the aircraft [13] [14]. The calculation of the gains for the controller was based only on the SISO TF identified by Pang (2018) [12]. They were subsequently evaluated in UM/NAST prior to flight. The control requirements for the PI controller implemented on the RRV are:

- Gain margin must be at least 6 dB and phase margin should be at least 60 degrees to ensure robustness of the closed-loop system.
- The crossover frequency for the angular (yaw and roll) rates should be set to 3 rad/s and for the roll angle to 1 rad/s as specified in [12].

### 3.1 Yaw Rate Regulator

The ESS for the yaw axis is based on a common yaw damper or yaw regulator [14]. The yaw rate regulator is shown in Fig. 3. The TF to relate the differential thrust to the yaw rate is defined by  $H_{\delta_{DT} \rightarrow r}$ . The ESS needs to read the value of the yaw rate and compare it to the commanded yaw rate ( $r_c$ ) given by the pilot. The error is then filtered by the proportional gain for yaw rate ( $K_{Pr}$ ) and the control signal sent to the actuators is  $u_{DT}$ .

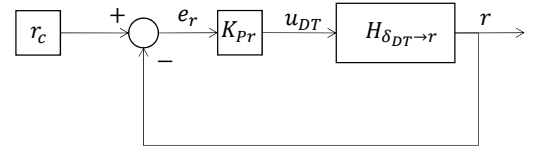


Fig. 3 Yaw rate ESS architecture.

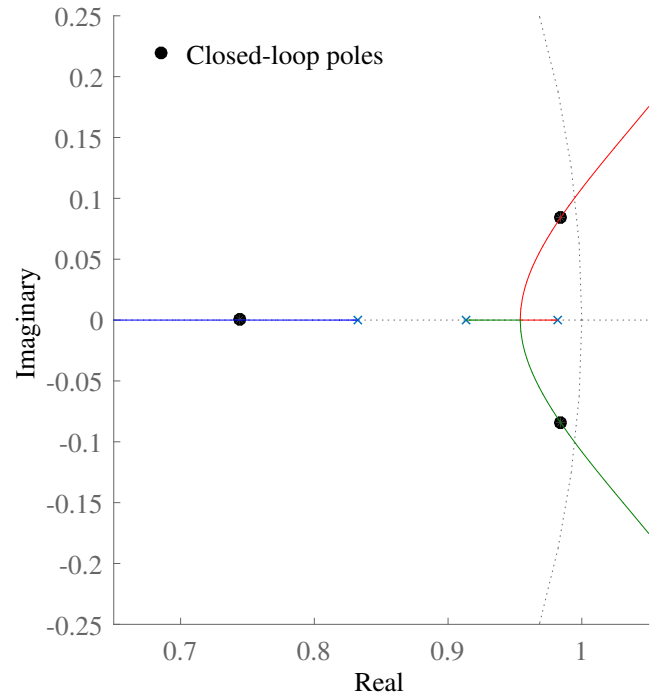


Fig. 4 Root locus and poles of the yaw rate regulator.

The calculation of the gains was based on the root locus plot. The identified discrete TF has a sampling time of 0.01 s. The stability of the



linear system is granted inside the unity circle. The poles of the closed-loop system were moved to achieved the ESS goal. Figure 4 shows the root locus of the yaw TF and the poles of closed-loop system for the yaw regulator.

The bode plot of the yaw rate closed-loop system is shown in Figure 5. It is possible to see that the system bandwidth cut frequency is 3 rad/s. The gain margin of the ESS is 13.8 dB and the phase margin is 87 degrees. The resultant gain is able to increase the damping of the system while satisfying the control requirements.

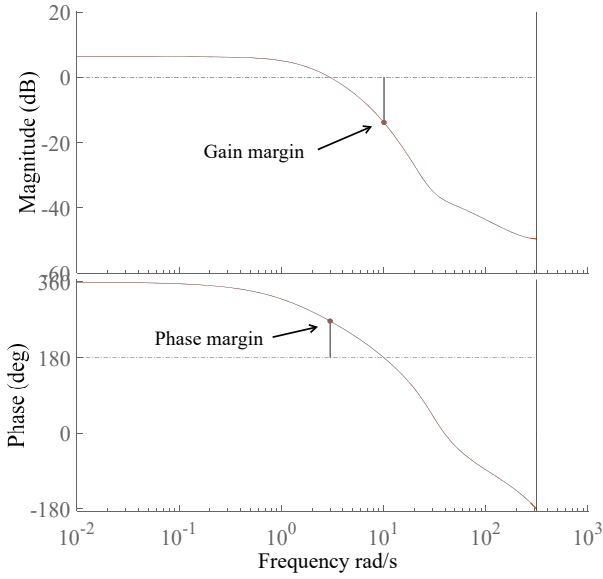


Fig. 5 Bode plot of the yaw rate ESS.

### 3.2 Roll Angle Tracker

The objective of the ESS in the roll axis is not only to ease the pilot workload by regulating the angular rate but also to act as a roll angle tracker to help the pilot automatically return the aircraft to a level flight condition. The roll angle tracker is shown in Fig. 6. The TF to relate the spoiler deflection to the roll rate is defined by  $H_{\delta_s \rightarrow p}$ . The system's inner-loop is a  $p$  tracker, the PI gain  $K_{PIp}$  is in charge of minimizing the error ( $e_p$ ) between the commanded roll rate ( $p_c$ ) and the measured  $p$ . Then, the outer-loop regulates the roll angle of the aircraft. The measured  $\phi$  is compared to the commanded roll angle ( $\phi_c$ ). The roll angle error ( $e_\phi$ ) is minimized by the proportional

roll angle gain ( $K_{P\phi}$ ). The output of  $K_{P\phi}$  is the commanded roll rate for the inner-loop. The final control signal for the spoilers is  $u_s$ .

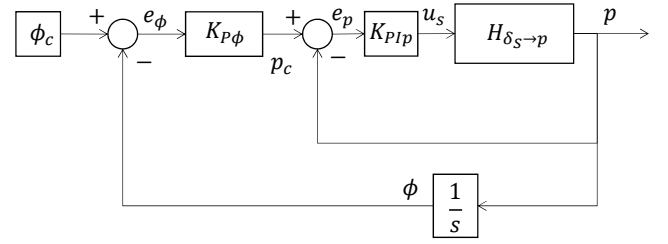


Fig. 6 Roll angle tracker architecture.

In this case, the root locus plot was also used to define the position of the poles of the system to attain the control requirements. Figure 7 shows the closed-loop root locus of the roll TF. The first step is to compute  $K_{PIp}$  to achieved the 3 rad/s bandwidth cut frequency. Once the tracking characteristics of the system are attained the outer-loop is calculated. It is possible to see how all poles of the closed-loop system are inside the unity circle.

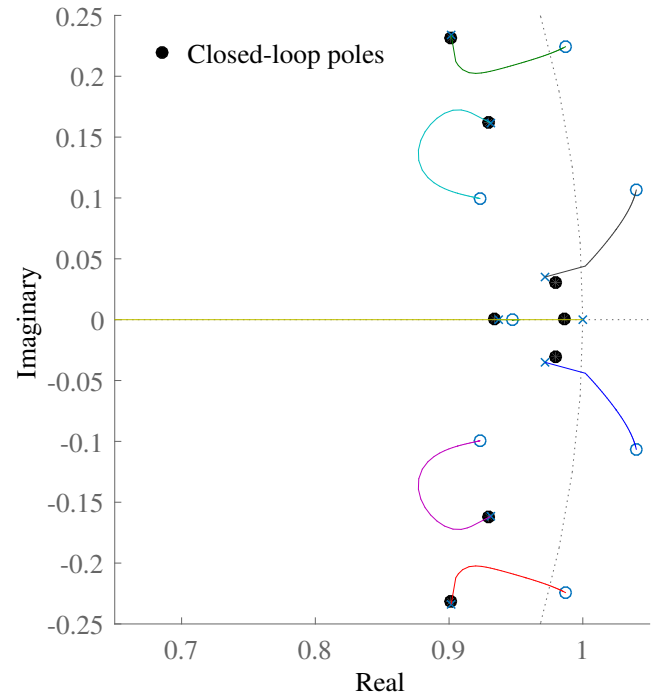
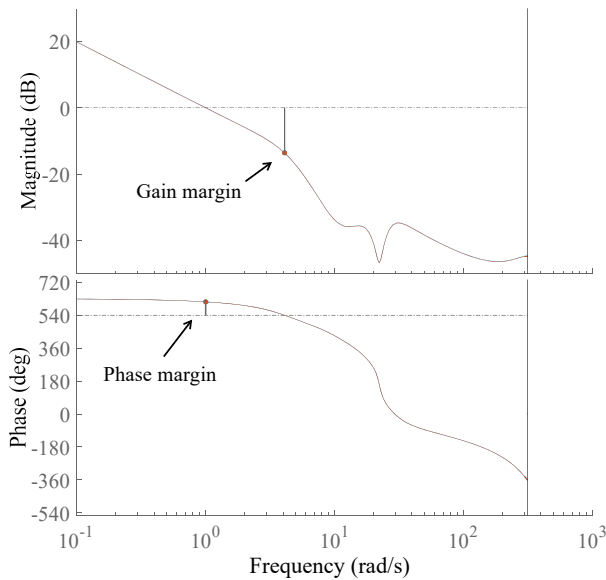


Fig. 7 Root locus and poles of the roll angle tracker.

Figure 8 shows the bode plot for the roll angle tracker. This plot includes the effect of the



**Fig. 8** Bode plot of the roll angle tracker.

inner-loop. It is possible to observe that the final closed-loop system has a bandwidth cut off frequency of 1 rad/s. The gain margin of the closed-loop system is 13.6 dB and the phase margin is 72.7 degrees.

#### 4 Flight Test Procedures

The flight testing area of operation is approximately 800 m by 500 m, with a maximum allowed altitude of operation of 122 m ( $\approx 400$  ft). The objective of the test was to evaluate the HQ of the aircraft in closed-loop. Perturbations were added in the form of doublets in the spoilers to excite the roll axis and as doublets in the differential thrust to excite the yaw axis.

The pilot took off with the ESS turned off. Once an operational height of 60 m ( $\approx 200$  ft) was achieved, the pilot establishes a race-track pattern and activates the ESS. Then he started to qualitatively assess the stability and controllability of the airplane performing altitude change and turn based maneuvers within the confines of the test site. Flight tests are limited to a duration of 12 min due to battery life. Figure 9 shows the RRV in operation during the flight test, showing visible wing deflection.

After the pilot has verified the adequate per-



**Fig. 9** X-HALE during flight.

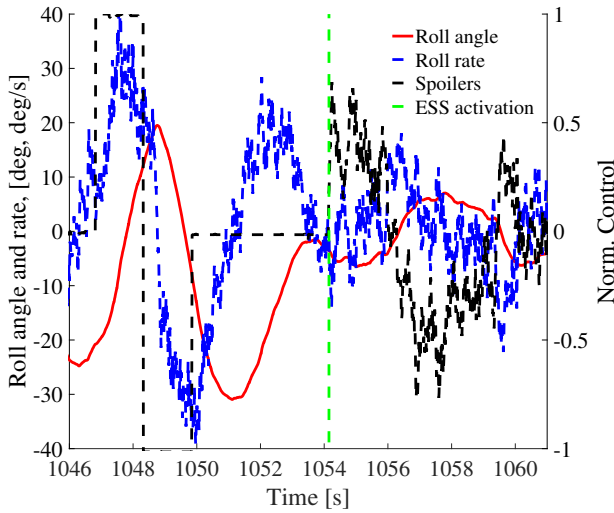
formance of the UAS with a tolerable pilot workload, the disturbance rejection evaluation was started. The goal is to demonstrate how the ESS is able to regulate and level the airplane after perturbation. The procedure for disturbance injection tests consists on taking the airplane to straight and level flight condition, deactivating the ESS, and injecting the doublet signal for 4 s. Once the doublet is completed the pilot must reactivate the ESS and command the aircraft back to straight and level condition.

#### 5 Results

Two sets of results are presented next that are directly connected to the use of PI controllers in VFA: (i) the performance assessment of the ESS and (ii) its impact on the aircraft's HQ.

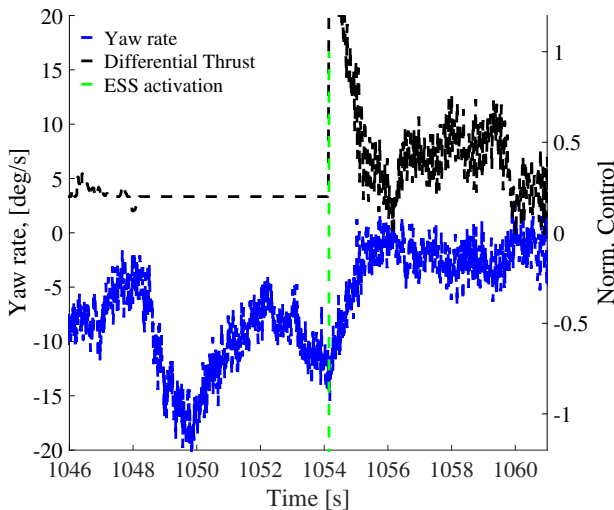
##### 5.1 ESS Performance Assessment

Figures 10 to 12 show the X-HALE response to a spoiler doublet. The control input has been normalized between  $-1$  and  $1$  to represent the limits of the actuators. The duration of the doublet is 3 s (1.5 s per side), the deflection of the spoiler goes from 0 to 25 degrees on each wing tip. The elevator deflection ranges from  $-25$  to 25 degrees. To be able to trim the aircraft, a normalized differential thrust of 0.2 is needed and the correction is sent from the Ground Station straight to the PixHawk through QGroundControl. No trim corrections are added by the pilot.



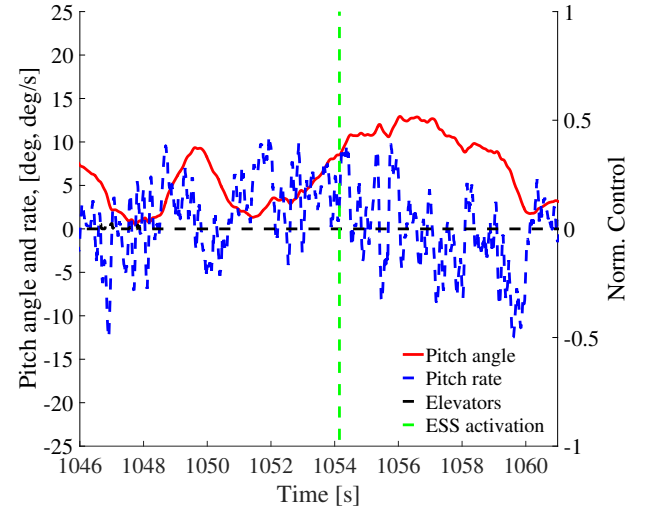
**Fig. 10** Roll response to a roll disturbance.

Figure 10 shows the roll response to a spoiler doublet. From it one can see that the aircraft responds to the perturbation by increasing the roll angle up to 20 degrees during the first half of the doublet. It is also possible to observe how the roll angle tends to increase even more in the next cycle, reaching 30 degrees after the doublet is completed. During this time, the pilot did not interfere with the flight. Once the ESS is activated (time 1054 s), the perturbation immediately starts to be damped. The differential thrust and the spoilers kick in to regulate  $\phi$ ,  $p$  and  $r$ .



**Fig. 11** Yaw response to a roll disturbance.

Figure 11 shows how the ESS was able to



**Fig. 12** Pitch response to a roll disturbance.

rapidly regulate the yaw rate. The yaw rate increased up to  $-20$  degrees/s during the roll perturbation.

The ESS commands the pair of outboard motors to full differential thrust for almost half second to compensate for the increase in yaw rate. It is possible to see how the differential thrust settles around its normalized trim position of 0.2 once the aircraft is regulated. In Fig. 12, it is possible to see that no elevator command was applied during the entire maneuver.

Figures 13 to 15 present the X-HALE's response to a differential thrust doublet. In this case the pilot activated the ESS 2 s after the doublet is finished. Figure 13 shows the large roll response after the perturbation. The second roll angle peak is greater than the first one, reaching almost 40 degrees. The damping action of the ESS can be clearly seen in this case. Both roll angle and rate are regulated to track the level wing condition. Once the ESS is activated (time 1266 s), the spoilers saturate to the full deflection position for a second until they are able to start to bring the aircraft back to level. The roll tracker was able to stabilize the aircraft and follow the zero angle reference.

It is possible to observe the differential thrust doublet in Fig. 14. As in the spoiler doublet case, the yaw rate is rapidly regulated once the ESS is turned on. Less control authority was required

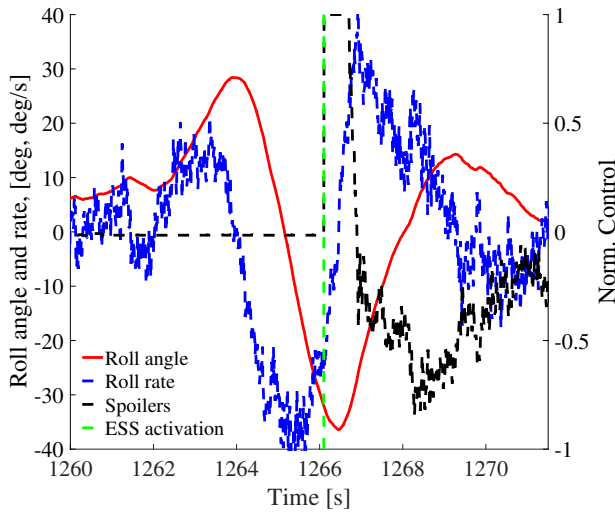


Fig. 13 Roll response to a yaw disturbance.

by the yaw rate regulator as compared to the roll perturbation case.

Figure 15 presents the pitch response. No major pitch excursions were developed in the pitch axis. The oscillation of the aircraft is kept between  $-5$  and  $10$  degrees. No pilot compensation was needed during the maneuver and the elevator was never activated.

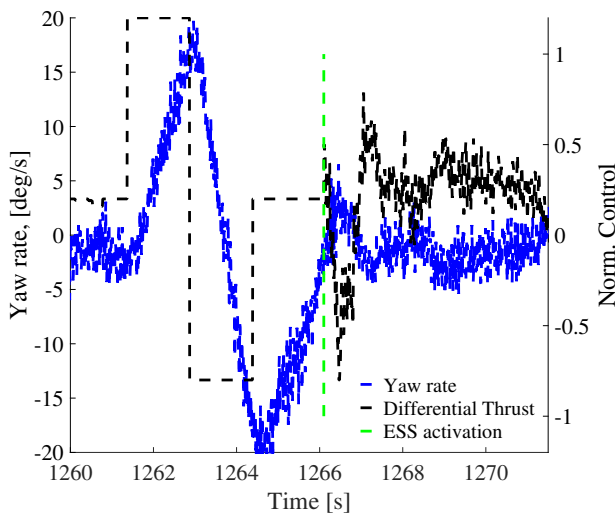


Fig. 14 Yaw response to a yaw disturbance.

## 5.2 Handling Qualities Evaluation

Once the aircraft safely landed, the pilot was surveyed through each flight phase and the overall flight. The pilot reported good control author-

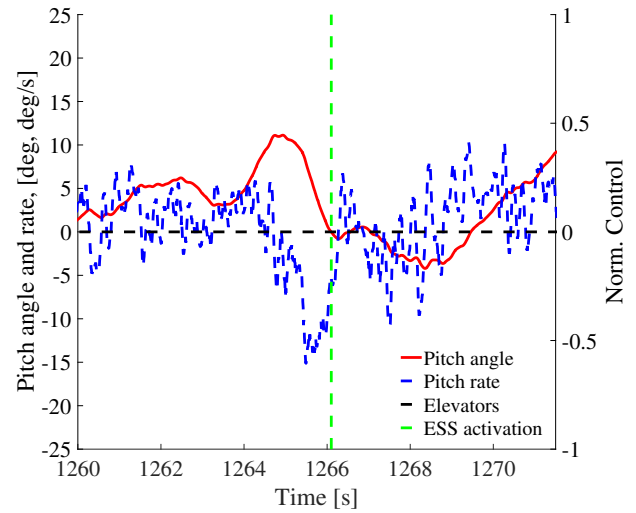


Fig. 15 Pitch response to a yaw disturbance.

ity during climb, descend, turn and land maneuvers. The pilot described the closed-loop aircraft as controllable and that it showed adequate performance attainable with a tolerable pilot workload. However, the pilot also pointed out that there is still some margin to improve the closed-loop system. The aircraft is capable of achieving the desired performance with moderate pilot compensation. The X-HALE with ESS activated was classified 4 in the Cooper-Harper rating scale when compared to a 9 without the ESS.

## 6 Conclusions

An enhanced stability system based on rigid body state measurements was designed for a very flexible aircraft. The control system was computed using identified transfer functions that include effects of the entire dynamics of the airplane. The X-HALE RRV was used as a testbed to evaluate the performance of the controller. A yaw rate damper was used to regulate the yaw axis. A reference roll tracking controller was implemented to guide the airplane back to a wing level position. Flight test results show that both control systems are able to regulate the aircraft after perturbations were injected and bring the X-HALE back to its trim condition.

Pilot evaluation was used to quantify the handling qualities of the X-HALE. The closed-loop system shows a significant improvement com-



pared to the open-loop response of the aircraft. The handling qualities of the X-HALE was rated 4 in the Cooper-Harper rating scale. From the pilot's evaluation, it is possible to affirm that the airplane with ESS is controllable sufficiently to ensure safe operation. This control system will be installed on the X-HALE ATV to initiate a more detailed system identification and obtain detailed in flight data of the coupled flight dynamics and aeroelastic response of the aircraft.

## References

- [1] Cesnik, C. E. S., Palacios, R. and Reichenbach E., Reexamined Structural Design Procedures for Very Flexible Aircraft. *Journal of Aircraft*. Vol. 51, No. 5, pp 1580-1591. (2014).
- [2] Cesnik, C. E. S., Senatore, P., Su, W., Atkins, E., Shearer, C., X-HALE: A Very Flexible Unmanned Aerial Vehicle for Nonlinear Aeroelastic Tests. *AIAA Journal*. Vol. 50, No. 12, pp 2820-2833. (2012).
- [3] Shearer, C. M. and Cesnik, C. E. S., Nonlinear flight dynamics of very flexible aircraft, *Journal of Aircraft*, Vol. 44, No. 5, pp. 1528-545, (2007).
- [4] Su, W. and Cesnik, C. E. S., Dynamic response of highly flexible flying wings, *AIAA journal*, Vol. 49, No. 2, pp. 324-339, (2011).
- [5] Pang, Z. Y., Cesnik, C. E. S., and Atkins, E. M., In-Flight Wing Deformation Measurement System for Small Unmanned Aerial Vehicles, *55th AIAA/ASME/ASCE/AHS/SC Structures, Structural Dynamics, and Materials Conference*, National Harbor, Maryland, (2014).
- [6] Jones, J. R. and Cesnik, C. E. S., Preliminary flight test correlations of the X-HALE aeroelastic experiment, *The Aeronautical Journal*, Vol. 119, No. 1217, pp. 855-870, (2015).
- [7] *Pixhawk Developer Manual*, <http://dev.px4.io>, Accessed: 2018-06-28
- [8] *QGroundControl User Guide*, <https://docs.qgroundcontrol.com/en/>, Accessed: 2018-06-28
- [9] Cooper, G. E., and Harper, R. P., The Use of Pilot Rating in the Evaluation of Aircraft Handling Qualities, *NASA TN-D5153*, (1969).
- [10] Silvestre, F. J., Guimaraes Neto, A. B., Bertolin, R. M., da Silva, R. G. A., and Paglione, P. Aircraft Control Based on Flexible Aircraft Dynamics. *Journal of Aircraft*. 54(1), pp. 262-271. (2016).
- [11] Rona, F., González, P. J., Silvestre, F. J., Cesnik, C. E. S., and Pang, Z. Y., Robustness Analysis of a Stability Augmentation System of a Highly Flexible Aircraft, *2018 AIAA Guidance, Navigation, and Control Conference*, Kissimmee, Florida, (2018).
- [12] Pang, Z. Y., *Modeling, Simulation and Control of Very Flexible Unmanned Aerial Vehicle*, Ph.D. Dissertation, University of Michigan, Ann Arbor, Michigan, (2018).
- [13] Blakelock, J. H., *Automatic Control of Aircraft and Missiles*, John Wiley & Sons, Inc., New York, New York, 2nd ed., (1991).
- [14] Nelson, R., *Flight Stability and Automatic Control*, The McGraw-Hill Companies, Inc., New York, New York, 2nd ed., (1998).

## 7 Acknowledgements

The authors would like to thank the X-HALE pilot, Keith Shaw, for his superb skills and support to flight tests, and Bilal Sharqi, John Hansen, and the rest of the X-HALE crew from the Active Aeroelasticity and Structures Research Laboratory for their support during the flight test campaign.

This work has been funded by the Center for Unmanned Aircraft Systems (C-UAS), a National Science Foundation Industry/University Cooperative Research Center (I/UCRC) under NSF Award No. 1738714 along with significant contributions from C-UAS industry members.

## 8 Contact Author Email Address

Mail to: [pedrojgonzalezr@gmail.com](mailto:pedrojgonzalezr@gmail.com).

## Copyright Statement

The authors confirm that they, and/or their company or organization, hold copyright on all of the original material included in this paper. The authors also confirm that they have obtained permission, from the copyright holder of any third party material included in this paper, to publish it as part of their paper. The

authors confirm that they give permission, or have obtained permission from the copyright holder of this paper, for the publication and distribution of this paper as part of the ICAS proceedings or as individual off-prints from the proceedings.